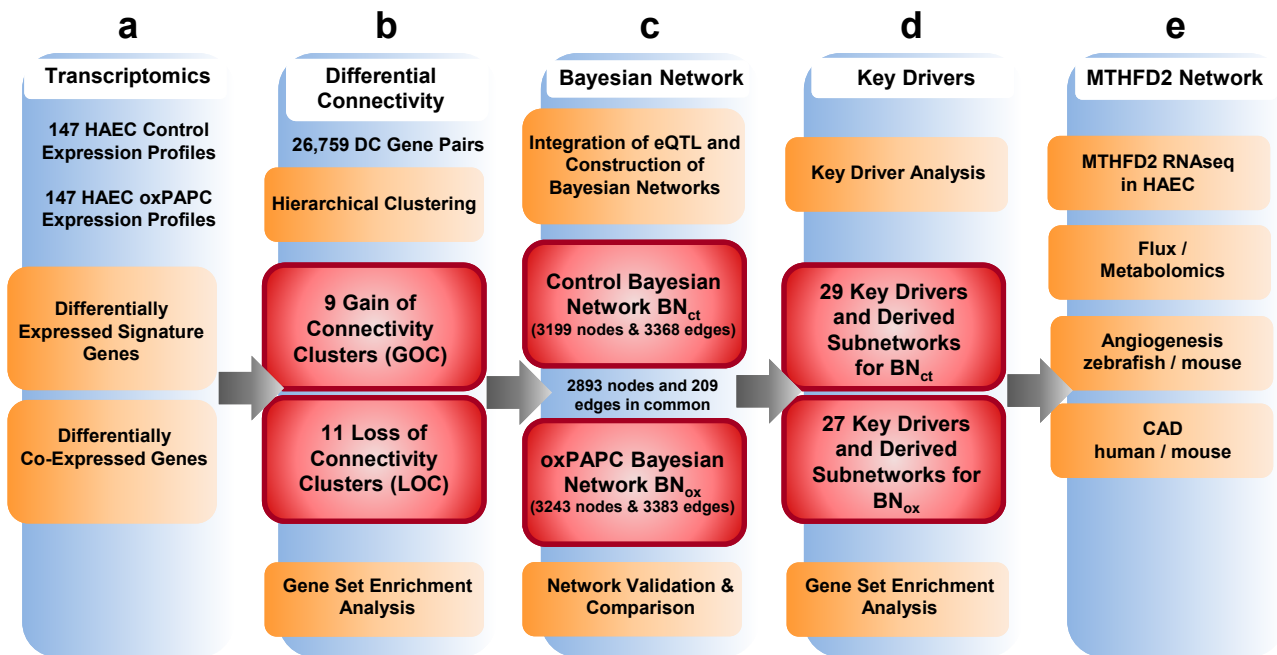


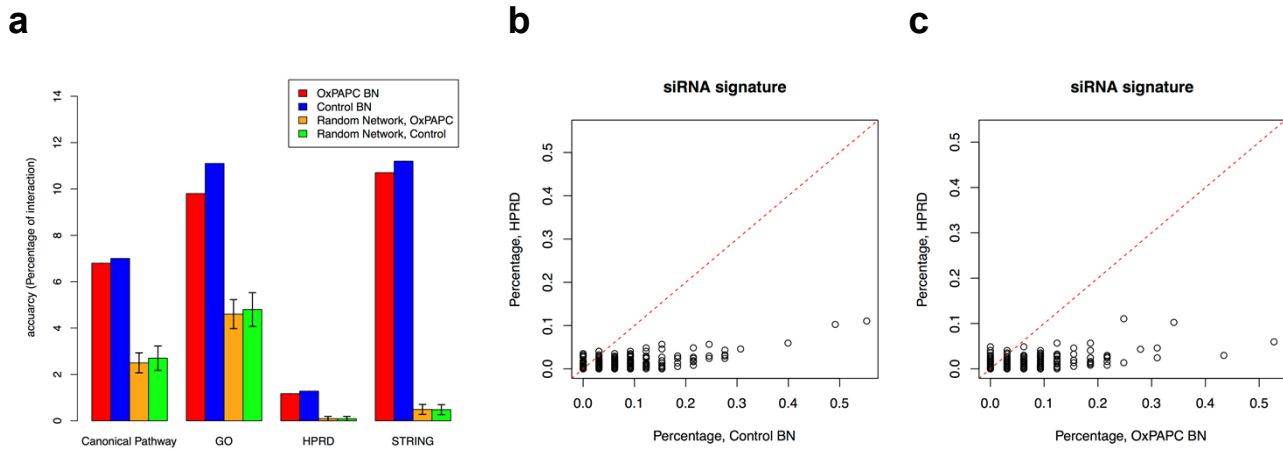
**Oxidized phospholipids regulate amino acid metabolism through MTHFD2 to facilitate nucleotide release in endothelial cells**

**Hitzel et al.**

## Supplementary Figures



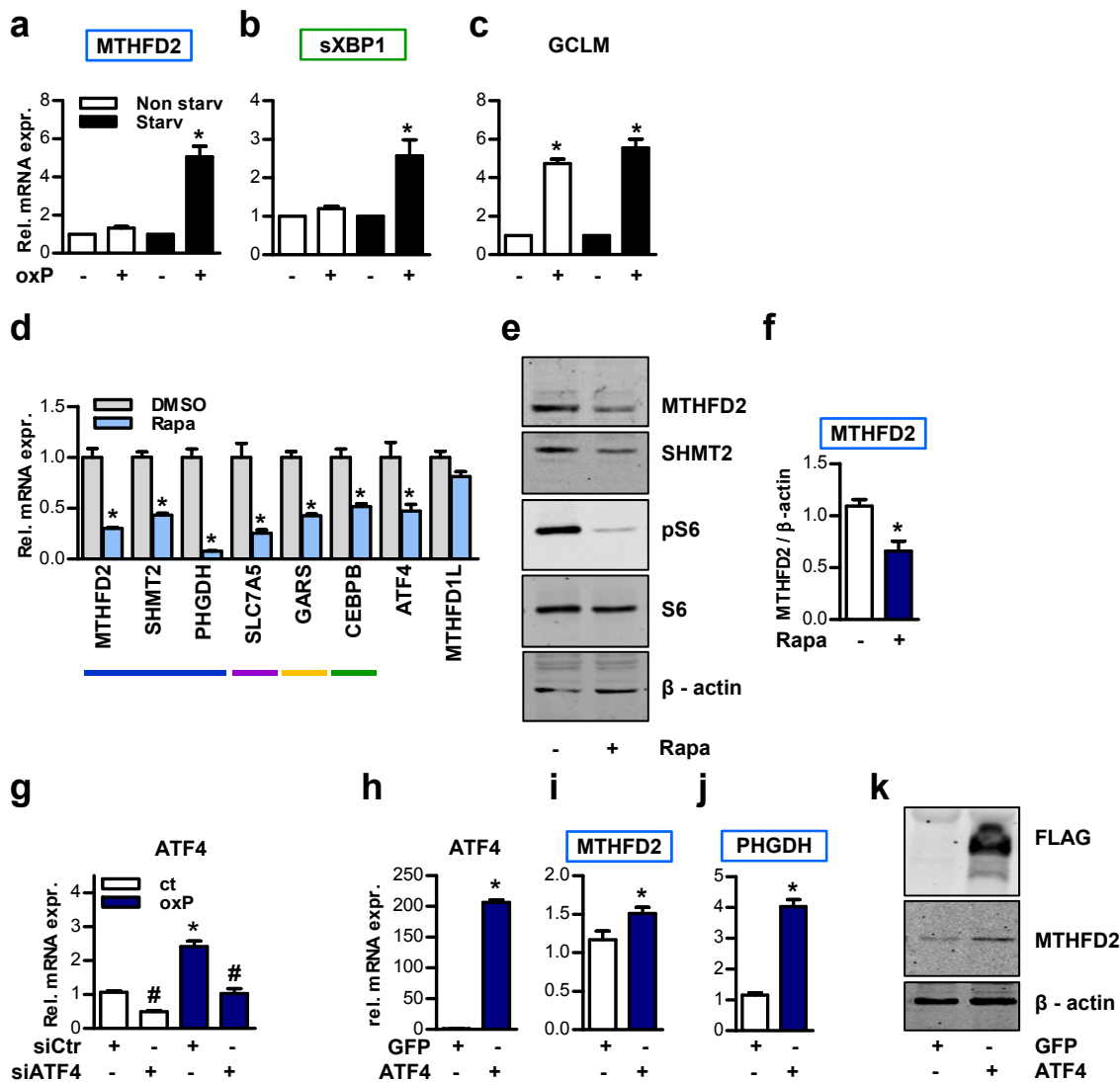
**Supplementary Figure 1 Integrative network approach in HAEC.** Expression profiles (a) were used to compute differential connectivity clusters (b) and genotype profiles were integrated to construct Bayesian networks (c). Key drivers of the Bayesian networks were identified (d) and the subnetwork of the key driver MTHFD2 was investigated in detail (e).



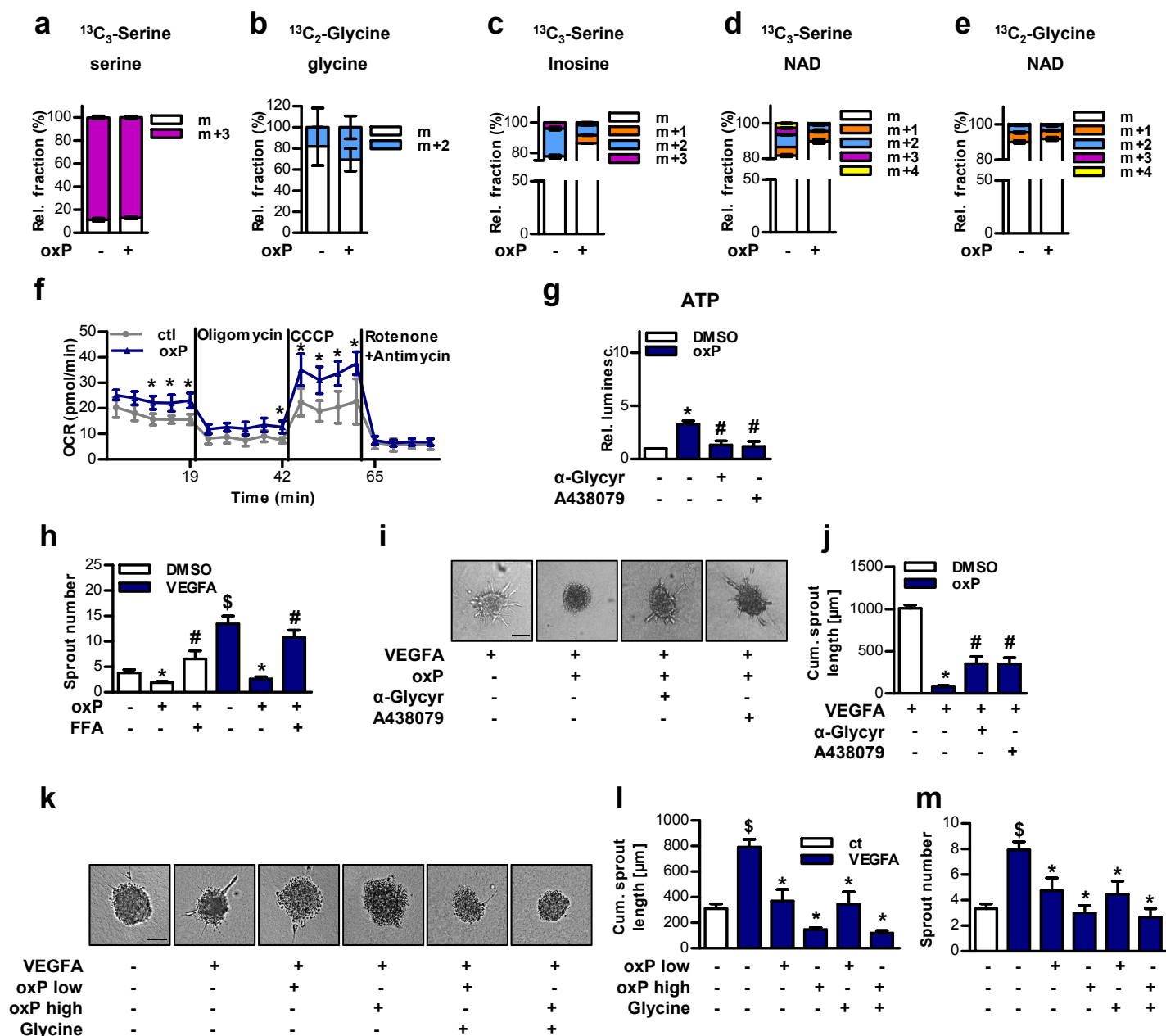
**Supplementary Figure 2 Assessment of HAEC Bayesian networks.** (a) Estimated accuracy of Bayesian networks (BN) based on four independent databases of gene networks and gene sets, including canonical pathway, Gene ontology (GO), Human Protein Reference Database (HPRD), and Search Tool for the Retrieval of Interacting Genes/Proteins database (STRING). The percentage of inferred gene-gene connections that are in existing protein/gene network databases is shown. For the random networks, the mean of accuracy is shown based on 100 random networks. For all the reference databases considered, the estimated accuracy of our Bayesian networks is significantly greater than random networks. (b), (c) Comparison of estimated accuracies for constructed Bayesian networks and HPRD networks. For each gene set that is significantly regulated by siRNA treatment in human umbilical vein endothelial cells, the percentage of inferred gene-gene connections that are within each gene set is shown based on our constructed control Bayesian network (x-axis) (b) or oxPAPC Bayesian network (x-axis) (c) and HPRD (y-axis).



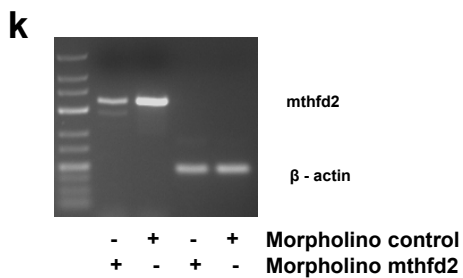
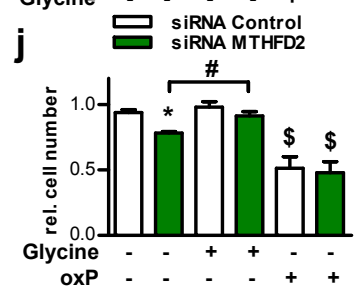
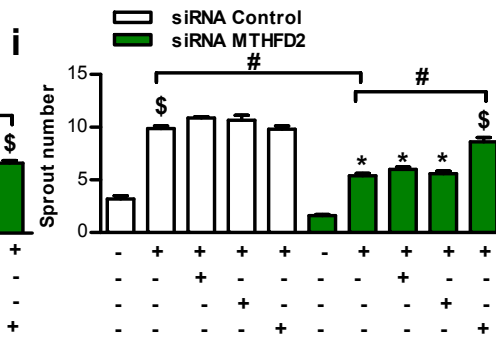
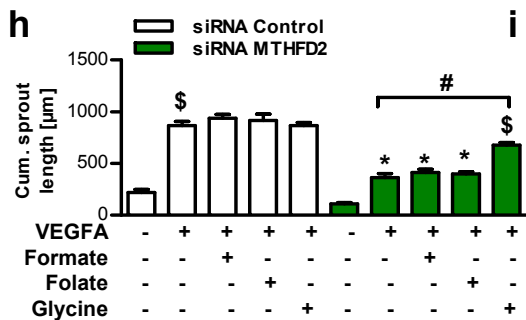
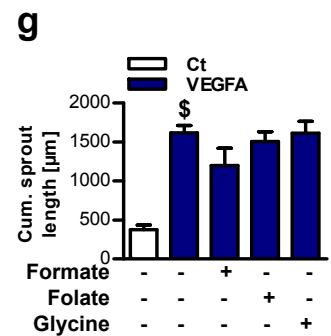
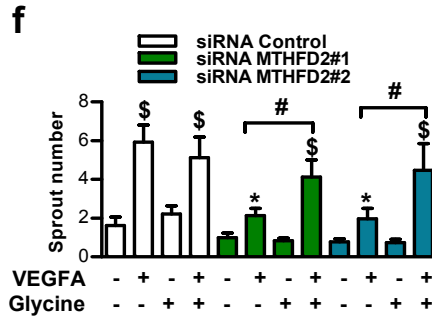
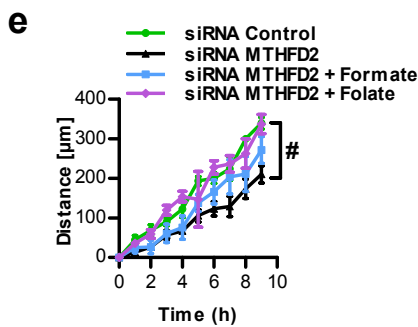
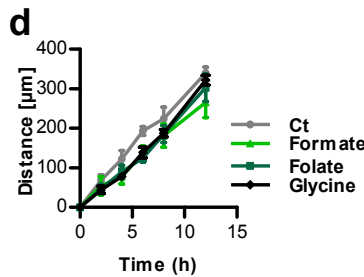
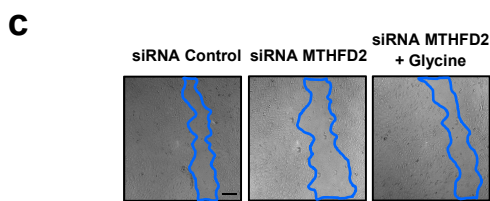
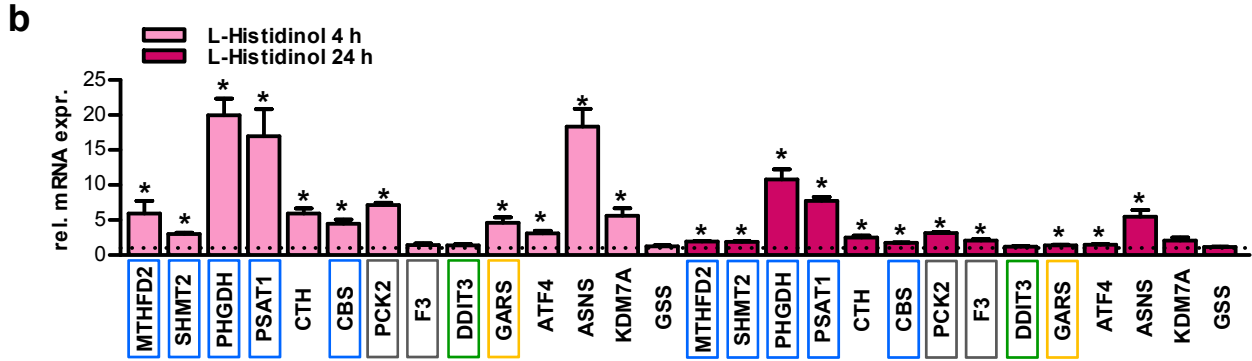
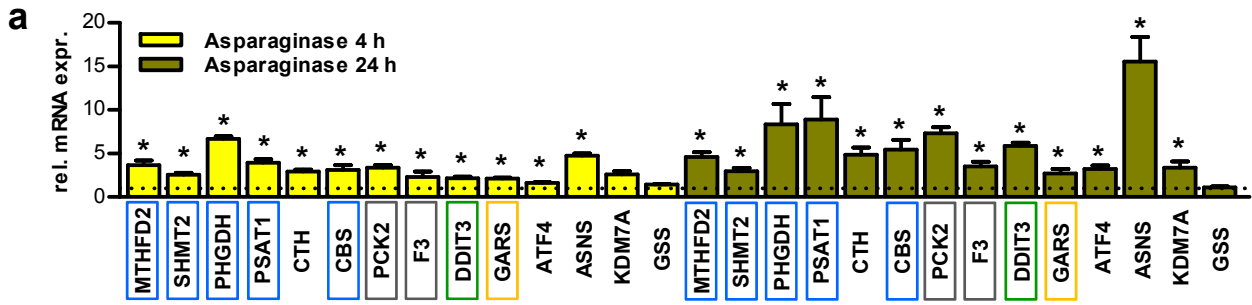
**Supplementary Figure 3 Canonical and non-canonical gene set enrichment.** Heatmap of P-values from selected canonical and non-canonical gene set categories (MSigDB) for *MTHFD2* RNAseq signature (FDR<0.05), amino acid cluster and *MTHFD2* network. *NFE2L2* = Nrf2 (Nuclear Factor, Erythroid 2 Like 2), *BMI1* = BMI1 Proto-Oncogene, Polycomb Ring Finger.



**Supplementary Figure 4 Regulatory pathways contributing to oxPAPC induced *MTHFD2* network expression.** (a)-(c) Quantitative RT-PCR detection. HAEC were exposed to growth medium (8% FCS) (Non starv) with or without oxPAPC (oxP) or basal medium (1% FCS) (Starv) with or without oxPAPC (n=4). Genes belonging to *MTHFD2* network are framed as in Fig. 3a. *sXBP1* = spliced X-Box Binding Protein 1, *GCLM* = Glutamate-Cysteine Ligase Modifier Subunit. (d) Relative mRNA expression of genes belonging to the *MTHFD2* network as well as *ATF4* and *MTHFD1L* in HAEC exposed to rapamycin in growth medium (Rapa, 20 nM) or DMSO for 16 h (n=12). Genes belonging to *MTHFD2* network are highlighted as in Fig. 3a. (e),(f) Western Blot detection (e) and quantification (f) of HAEC treated with rapamycin in growth medium (20 nM) or DMSO for 16 h (n=4). (\* $P \leq 0.05$ , Student's t-test) (g) qRT-PCR detection of *ATF4* in HAEC treated as in Fig. 4 (j). (h)-(j) Relative mRNA expression in HAEC overexpressing GFP or Flag-tagged *ATF4* for 24 h (n=4). (\* $P \leq 0.05$ , Student's t-test) (k) Western Blot analysis of *MTHFD2* in HAEC overexpressing FLAG-tagged *ATF4* or GFP empty vector as control for 24 h. Data are represented as mean  $\pm$  SEM, \* $P \leq 0.05$ , # $P \leq 0.05$  (*ATF4* vs Control siRNA) (ANOVA with Bonferroni post-hoc test if not otherwise indicated).

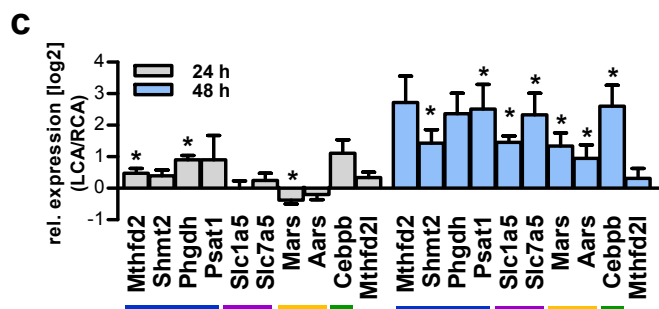
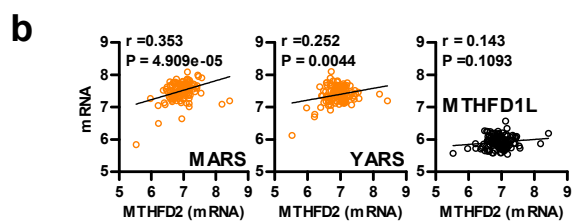
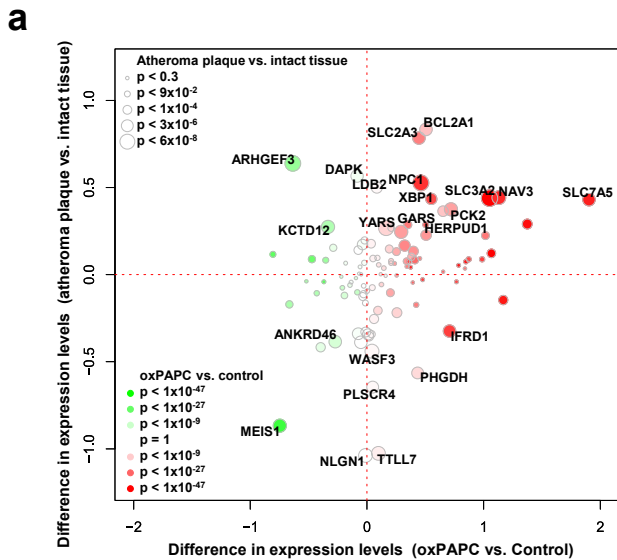


**Supplementary Figure 5 Vnut inhibitors rescue normal sprouting after oxPAPC treatment.** (a),(b) HAEC were treated with  $^{13}\text{C}_3$ -serine (a) or  $^{13}\text{C}_2$ -glycine (b) and oxPAPC (oxP) or control for 24 h and cells were lysed and measured by mass spectrometry (n=3). Relative fractions of intracellular non-heavy serine (m) or imported heavy-serine (m+3) (a) and relative intracellular fractions of non-heavy glycine (m) and imported heavy-glycine (m+2) (b) are shown. (c)-(e) HAEC were treated with  $^{13}\text{C}_3$ -serine (c),(d) or  $^{13}\text{C}_2$ -glycine (e) and oxPAPC or control for 24 h and supernatants were measured by mass spectrometry (n=3). Relative fractions of extracellular purine derivatives inosine (c) and NAD (d),(e) containing no (m), one (m+1), two (m+2), three (m+3) or four (m+4) heavy carbons are shown. (f) Oxygen consumption rate (OCR) profile as an index of mitochondrial respiration in HAEC exposed for 4 h to medium (1% FCS) with or without oxPAPC (n $\geq$ 3). HAEC were treated with the ATP synthase inhibitor Oligomycin (2.5  $\mu\text{M}$ ), with CCCP (1  $\mu\text{M}$ ) for maximal mitochondrial capacity and with antimycin A (1  $\mu\text{g/ml}$ ) and rotenone (1  $\mu\text{M}$ ) to inhibit mitochondrial activity. (ANOVA with repeated measures) (g) ATP measurement of supernatants of HAEC exposed to medium (1% FCS) with or without oxPAPC and  $\alpha$ -glycyrhretinic acid (50  $\mu\text{M}$ ) or A438079 (100  $\mu\text{M}$ ) for 8 hours. ATP was measured by luminescence and was normalized to the intracellular RNA concentration (n $\geq$ 3). (h) Sprout number in the spheroid outgrowth assay in Fig. 5p of human umbilical vein endothelial cells treated with combinations of oxPAPC, flufenamic acid (FFA, 50  $\mu\text{M}$ ) and VEGF-A165 (10 ng ml $^{-1}$ ) as indicated (n=6). (i),(j) Spheroid assay (i) and quantification (j) of the cumulative sprout length of human umbilical vein endothelial cells treated with oxPAPC,  $\alpha$ -glycyrhretinic acid (50  $\mu\text{M}$ ) or A438079 (100  $\mu\text{M}$ ) as indicated. All samples were treated with VEGF-A165 (10 ng ml $^{-1}$ ) (n=3). Scale bar: 50  $\mu\text{M}$ . (k)-(m) Spheroid assay (k) and quantification of the cumulative sprout length (l) and sprout number (m) of human umbilical vein endothelial cells treated with low oxPAPC concentration, high oxPAPC concentration, glycine (500  $\mu\text{M}$ ) and VEGF-A165 (10 ng/ml) as indicated (n=6). Scale bar: 50  $\mu\text{M}$ . Data are represented as mean  $\pm$  SEM, \*P  $\leq$  0.05 (oxP vs Ct), #P  $\leq$  0.05 (inhibitor present vs absent), \$P  $\leq$  0.05 (VEGFA vs Ct), (ANOVA with Bonferroni post-hoc test if not otherwise indicated).



**Supplementary Figure 6 Impact of amino acid and folate metabolism on endothelial cells. (a)** Quantitative RT-PCR detection. HAEC were treated with 1 U ml<sup>-1</sup> Asparaginase (ASNase) or H<sub>2</sub>O in growth medium for 4 and 24 hours (n≥4). Genes belonging to *MTHFD2* network are framed as in Fig. 3a. *CTH* = cystathionine gamma-lyase, *CBS* = cystathionine-beta-synthase, *F3* = Coagulation factor III / tissue factor, *ASNS* = asparagine synthetase, *KDM7A* = Lysine Demethylase 7A, *GSS* = Glutathione Synthetase. **(b)** Quantitative RT-PCR detection. HAEC were treated with L-Histidinol (2 μM) or H<sub>2</sub>O in growth medium for 4 and 24 hours (n≥4). Genes belonging to *MTHFD2* network are framed as in Fig. 3a. **(c)** Representative image of migration scratch wound assay in Fig. 6g. Scale bar: 100 μM. **(d)** Migration distance in a scratch wound assay of human umbilical vein endothelial cells treated with formate (50 μM), folate (10 μM) or glycine (500 μM) for the indicated time points (n=3). **(e)** Migration as in (d) of human umbilical vein endothelial cells treated with siRNA against scramble control or *MTHFD2* (n=3). (Anova with repeated measures) **(f)** Quantification of sprout number of spheroid assay in Fig. 6h (n=6). **(g)** Quantification of the cumulative sprout length of a spheroid assay in human umbilical vein endothelial cells treated with formate (50 μM), folate (10 μM), glycine (500 μM) and VEGF-A165 (10 ng ml<sup>-1</sup>) as indicated (n=8). **(h),(i)** Quantification of cumulative sprout length (h) and sprout number (i) of spheroid assay as in (g). Human umbilical vein endothelial cells were additionally treated with siRNA against scramble control or *MTHFD2* (n=3). **(j)** Relative cell number of human umbilical vein endothelial cells treated with glycine (500 μM) or oxPAPC for 24h. Cells were counted 48 h after transfection with scramble control or *MTHFD2* siRNA (n≥6). **(k)** RT-PCR for *mthfd2* and β-actin in *tg(fli1:EGFP)* embryos at 72 hours post-fertilization injected with control or *mthfd2* morpholino at 0.5 hours post-fertilization. One single experiment is shown. Data are represented as mean ± SEM, \*P ≤ 0.05 (*MTHFD2* vs Control siRNA), #P ≤ 0.05 (with vs without amino acid or folate), §P ≤ 0.05 (VEGFA or oxP vs Ct) (ANOVA with Bonferroni post-hoc test).





**Supplementary Figure 7 Expression of *MTHFD2* network in cardiovascular disease models. (a)** Expression of genes in *MTHFD2* network in human aortic plaques. Difference in expression levels of genes in *MTHFD2* network in 32 human atheroma plaques compared to 147 oxPAPC treated HAEC. **(b)** Scatter plots (additional to Fig. 7b) showing expression correlation in 126 human carotid plaque samples between *MTHFD2* and the *MTHFD2* network genes *MARS* and *YARS* (colored according to Fig 3a) as calculated by Pearson correlation. There was no correlation with the non-*MTHFD2* network gene *MTHFD1L* **(c)** Log<sub>2</sub> expression profiles of representative genes within the *MTHFD2* network in the endothelium of healthy right carotid artery (RCA) compared to partially ligated left carotid artery (LCA) 24 h and 48 h weeks post ligation (n=5). Genes belonging to *MTHFD2* network are highlighted as in Fig. 3a. Data are represented as mean  $\pm$  SEM, \* $P \leq 0.05$  (ANOVA with Bonferroni post-hoc test).

**Fig. 4h**

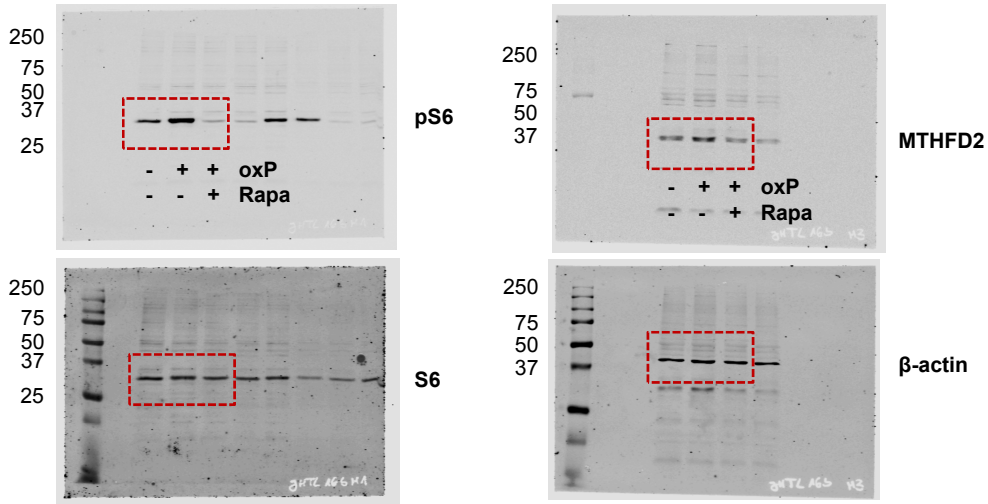


**Fig. 7e**

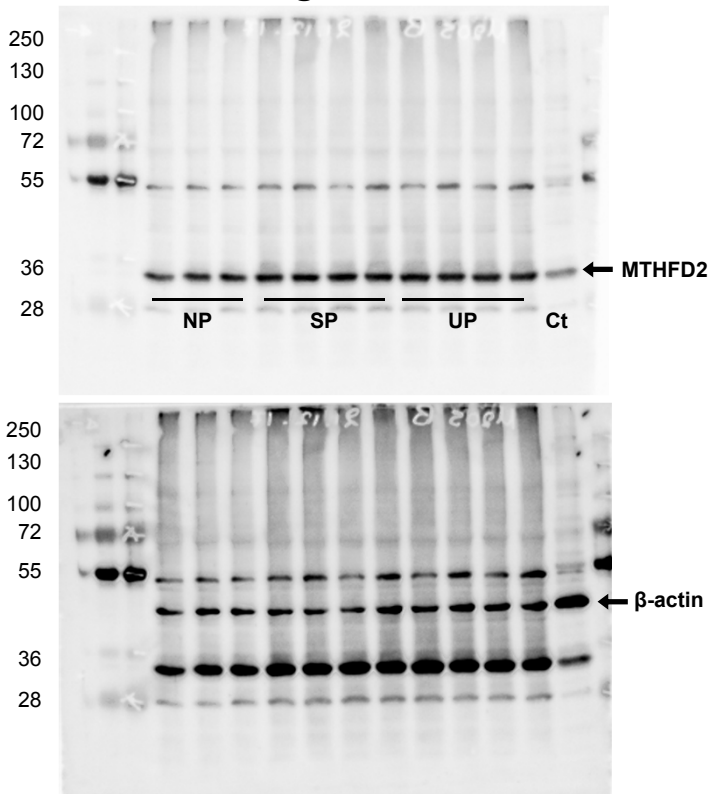
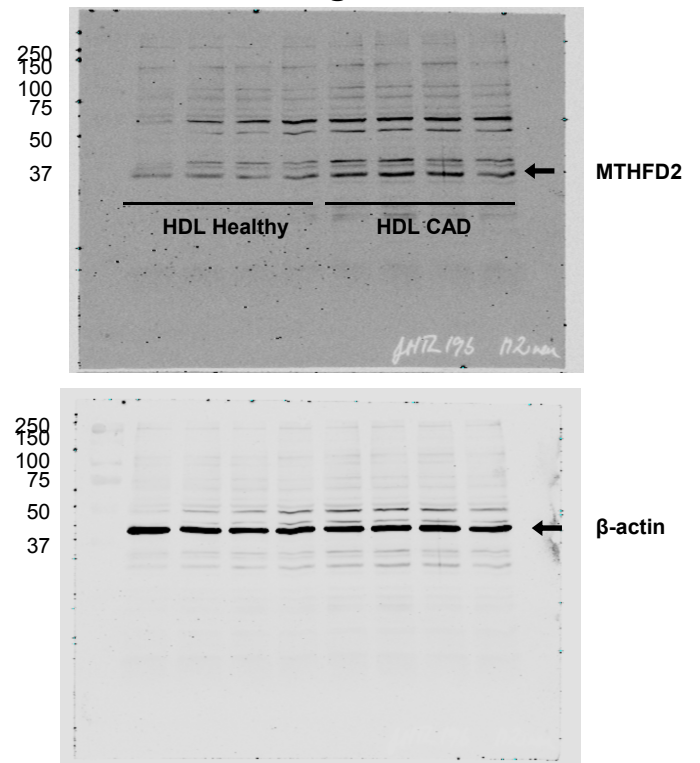


**Fig. 7r**



**Supplementary Figure 8 Full scans of Western Blots.**

## Supplementary Tables

**Supplementary Table 1 Canonical pathway enrichment in gain of connectivity clusters.**

<b>GOC cluster</b>	<b>Top functional category</b>	<b>p-value</b>
<b>GOC1</b>	GO_MACROAUTOPHAGY	2.55E-03
<b>GOC2</b>	GO_HOMOPHILIC_CELL_ADHESION_VIA_PLASMA_MEMBRANE_ADHESION_MOLE	3.22E-34
	CULES KEGG_LYSOSOME	2.21E-10
<b>GOC3</b>	GO_LAMELLIPODIUM	1.81E-05
<b>GOC4</b>	GO_MITOTIC_CELL_CYCLE	2.12E-31
	HALLMARK_G2M_CHECKPOINT	1.11E-21
	REACTOME_CELL_CYCLE	4.35E-19
	KEGG_CELL_CYCLE	2.06E-05
<b>GOC5</b>	GO_NEGATIVE_REGULATION_OF_MITOTIC_CELL_CYCLE	7.74E-05
<b>GOC6</b>	GO_CELLULAR_AMINO_ACID_METABOLIC_PROCESS	1.63E-09
	HALLMARK_MTORC1_SIGNALING	2.66E-11
	REACTOME_CYTOSOLIC_TRNA_AMINOACYLATION	4.24E-09
	KEGG_AMINOACYL_TRNA_BIOSYNTHESIS	1.19E-08
<b>GOC7</b>	GO_ORGAN_MORPHOGENESIS	8.13E-08
<b>GOC8</b>	GO_NUCLEIC_ACID_BINDING_TRANSCRIPTION_FACTOR_ACTIVITY	6.28E-08
<b>GOC9</b>	GO_REGULATION_OF_CELLULAR_RESPONSE_TO_HEAT	6.33E-10

The top functional GO category and the top functional categories from KEGG, HALLMARK and REACTOME gene sets (if  $P$ -value  $\leq 1E-05$ ) of each gain of connectivity (GOC) cluster are listed.

Clusters are colored according to Fig. 1a.

**Supplementary Table 2 Canonical pathway enrichment in loss of connectivity clusters.**

LOC cluster	Top functional category	p-value
LOC1	GO_REGULATION_OF_MESODERM_DEVELOPMENT	2.91E-05
	HALLMARK_ESTROGEN_RESPONSE_LATE	5.49E-05
LOC2	GO_POSTTRANSCRIPTIONAL_REGULATION_OF_GENE_EXPRESSION	1.96E-06
	HALLMARK_P53_PATHWAY	3.66E-07
LOC3	GO_CATABOLIC_PROCESS	6.59E-07
	REACTOME_METABOLISM_OF_RNA	9.46E-05
LOC4	GO_DNA_DEPENDENT_DNA_REPLICATION	2.49E-09
	REACTOME_CELL_CYCLE	4.18E-09
	HALLMARK_E2F_TARGETS	1.17E-08
	KEGG_DNA_REPLICATION	7.28E-05
LOC5	GO_MITOCHONDRIAL_PART	2.01E-10
	HALLMARK_MYC_TARGETS_V1	5.02E-10
	REACTOME_CELL_CYCLE	4.29E-07
LOC6	GO_SPHINGOLIPID_METABOLIC_PROCESS	1.09E-04
LOC7	GO_REGULATION_OF_CELLULAR_AMIDE_METABOLIC_PROCESS	1.81E-06
	HALLMARK_TNFA_SIGNALING_VIA_NFKB	3.01E-06
LOC8	GO_RIBONUCLEOTIDE_BINDING	2.39E-09
	HALLMARK_G2M_CHECKPOINT	9.23E-11
LOC9	GO_NCRNA_PROCESSING	2.65E-09
	REACTOME_SRP_DEPENDENT_COTRANSLATIONAL_PROTEIN_TARGETING_TO_M	3.61E-08
	EMBRANE	9.28E-07
	KEGG_RIBOSOME	
LOC10	GO_IMMUNE_SYSTEM_PROCESS	1.40E-07
	KEGG_CELL_ADHESION_MOLECULES_CAMS	1.41E-06
	REACTOME_IMMUNOREGULATORY_INTERACTIONS_BETWEEN_A_LYMPHOID_AN	8.34E-05
	D_A_NON_LYMPHOID_CELL	
LOC11	GO_CIRCULATORY_SYSTEM_DEVELOPMENT	3.90E-12
	HALLMARK_TGF_BETA_SIGNALING	1.18E-06
	KEGG_TGF_BETA_SIGNALING_PATHWAY	2.17E-06

The top functional GO category and the top functional categories from KEGG, HALLMARK and REACTOME gene sets (if  $P$ -value  $\leq 1E-05$ ) of each loss of connectivity (LOC) cluster are listed.

Clusters are colored according to Fig. 1b.

**Supplementary Table 3 Canonical pathway enrichment in amino acid cluster.**

<b>Amino acid cluster: Top functional canonical gene set categories</b>	<b>p-value</b>
MTOR_UP.N4.V1_UP	4.74E-14
ALK_DN.V1_UP	3.24E-12
HALLMARK_MTORC1_SIGNALING	2.66E-11
HALLMARK_UNFOLDED_PROTEIN_RESPONSE	1.07E-09
GO_CELLULAR_AMINO_ACID_METABOLIC_PROCESS	1.63E-09
REACTOME_CYTOSOLIC_TRNA_AMINOACYLATION	4.24E-09
GO_ORGANIC_ACID_METABOLIC_PROCESS	8.75E-09
KEGG_AMINOACYL_TRNA_BIOSYNTHESIS	1.19E-08
REACTOME_TRNA_AMINOACYLATION	1.19E-08
TGANTCA_AP1_C	3.83E-08
RCGCANGCGY_NRF1_Q6	4.61E-08
GO_NEGATIVE_REGULATION_OF_CELL_DEATH	5.55E-08

The top 12 canonical gene sets and *P*-value are shown. *MTOR* = mechanistic Target of Rapamycin, *ALK* = Anaplastic Lymphoma Kinase, *AP1* = Activator protein 1, *NRF1* = Nuclear Respiratory Factor 1.

**Supplementary Table 4 Extended list of key driver subnetworks in control Bayesian network (Fig. 2a).**

<b>KD</b>	<b>size</b>	<b>Top functional canonical gene set category</b>	<b>p-value</b>
CDCA3	589	GO_DNA_REPLICATION	6.58E-19
PDSS1	544	GO_RIBOSOME_BIOGENESIS	5.83E-10
DOCK9	348	GO_INORGANIC_ION_TRANSMEMBRANE_TRANSPORT	5.85E-06
NEK2	317	HALLMARK_E2F_TARGETS	5.28E-24
TRAM1	281	KEGG_WNT_SIGNALING_PATHWAY	4.73E-05
TBC1D8	268	GO_INORGANIC_ION_TRANSMEMBRANE_TRANSPORT	8.52E-05
EMG1	243	GO_TRNA_PROCESSING	1.13E-04
CKS1B	232	GO_DNA_REPLICATION	7.56E-29
ITGAV	230	HALLMARK_INFLAMMATORY_RESPONSE	1.70E-06
PBK	223	GO_DNA_REPLICATION	2.86E-19
UBXN4	210	KEGG_WNT_SIGNALING_PATHWAY	4.95E-05
TIPIN	179	GO_ANTIGEN_PROCESSING_AND_PRESENTATION_VIA_MHC_CLASS_IB	6.61E-04
TMOD3	158	GO_REGULATION_OF_RNA_SPLICING	5.72E-05
GINS1	151	GO_DNA_REPLICATION	2.67E-20
PPM1F	150	GO_MEMBRANE_REGION	1.05E-05
DUT	143	GO_L_ASCORBIC_ACID_BINDING	4.05E-04
CDC20	141	GO_PEPTIDYL_TYROSINE_MODIFICATION	4.74E-04
TPP1	140	GO_VACUOLAR_LUMEN	1.76E-06
UCHL5	139	GO_RESPONSE_TO_TOPOLOGICALLY_INCORRECT_PROTEIN	7.36E-04
TAF9B	131	GO_TRANSCRIPTION_FACTOR_COMPLEX	5.06E-05
SERPINE1	127	GO_REGULATION_OF_N_METHYL_D_ASPARTATE_SELECTIVE_Glutamate_RECEPTOR_ACTIVITY	6.12E-05
KDR	125	GO_MEMBRANE_REGION	6.99E-07
SGSM2	122	REACTOME_UNFOLDED_PROTEIN_RESPONSE	3.92E-04
MRT04	119	GO_RIBOSOME_BIOGENESIS	6.91E-07
SFRS1	112	GO_POSITIVE_REGULATION_OF_GENE_EXPRESSION	2.01E-04
PGF	111	GO_TRIGLYCERIDE_CATABOLIC_PROCESS	1.59E-04
NISCH	110	REACTOME_UNFOLDED_PROTEIN_RESPONSE	2.06E-04
RBBP4	109	GO_EXECUTION_PHASE_OF_APOPTOSIS	2.14E-04
TSPAN7	100	GO_IMPORT_INTO_CELL	2.51E-04

Key driver subnetworks in control Bayesian network with most top ranked key driver (KD) of subnetwork, number of nodes (size), most significantly overrepresented functional category and *P*-value.

**Supplementary Table 5 Extended list of key driver subnetworks in oxPAPC Bayesian network (Fig. 2b).**

<b>KD</b>	<b>size</b>	<b>Top functional canonical gene set category</b>	<b>p-value</b>
<b>CCNB2</b>	513	HALLMARK_E2F_TARGETS	1.52E-20
<b>UBXN4</b>	318	GO_GOLGI_ORGANIZATION	2.85E-05
<b>KIF4A</b>	304	GO_CELL_CYCLE_PROCESS	3.52E-14
<b>NDC80</b>	263	HALLMARK_E2F_TARGETS	2.72E-14
<b>PCDH12</b>	261	GO_ANGIOGENESIS	4.85E-05
<b>ASPM</b>	242	GO_ORGANELLE_FISSION	1.96E-09
<b>CCNB1</b>	235	GO_ANION_TRANSMEMBRANE_TRANSPORTING_ATPASE_ACTIVITY	3.76E-04
<b>KDR</b>	214	HALLMARK_ESTROGEN_RESPONSE_LATE	1.96E-04
<b>CDCA3</b>	184	KEGG_ABC_TRANSPORTERS	1.12E-05
<b>NUSAP1</b>	175	GO_DNA_REPLICATION	2.71E-14
<b>PLK1</b>	160	GO_ANION_TRANSMEMBRANE_TRANSPORTING_ATPASE_ACTIVITY	1.18E-04
<b>CDKN3</b>	159	GO_ANION_TRANSMEMBRANE_TRANSPORTING_ATPASE_ACTIVITY	1.16E-04
<b>DPYSL2</b>	155	GO_IRON_ION_HOMEOSTASIS	6.65E-04
<b>LOC100292189</b>	139	GO_CIRCULATORY_SYSTEM_DEVELOPMENT	2.22E-04
<b>GRN</b>	138	KEGG_LYSOSOME	8.22E-11
<b>KIAA1462</b>	136	GO_REGULATION_OF_PHOSPHORUS_METABOLIC_PROCESS	3.95E-06
<b>TMED2</b>	131	GO_ACTIVATION_OF_NF_KAPPAB_INDUCING_KINASE_ACTIVITY	6.07E-04
<b>DNAJB1</b>	129	GO_PROTEIN_FOLDING	6.55E-07
<b>EMG1</b>	129	GO_NCRNA_PROCESSING	3.68E-05
<b>ASNS</b>	121	GO_CELLULAR_AMINO_ACID_METABOLIC_PROCESS	2.38E-09
<b>MTHFD2</b>	114	GO_CELLULAR_AMINO_ACID_METABOLIC_PROCESS	7.32E-08
<b>PNMA2</b>	114	GO_CIRCULATORY_SYSTEM_DEVELOPMENT	5.13E-04
<b>YWHAZ</b>	113	BIOCARTA_ARAP_PATHWAY	3.92E-04
<b>HSPA1A</b>	111	GO_PROTEIN_FOLDING	6.34E-06
<b>ARMCX2</b>	109	GO_CIRCULATORY_SYSTEM_DEVELOPMENT	2.71E-04
<b>CHAC1</b>	107	REACTOME_CYTOSOLIC_TRNA_AMINOACYLATION	2.98E-08
<b>SYPL1</b>	102	GO_NEGATIVE_REGULATION_OF_ERBB_SIGNALING_PATHWAY	5.86E-05

Key driver subnetworks in oxPAPC Bayesian networks with most top ranked key driver (KD) of subnetwork, number of nodes (size), most significantly overrepresented functional category and *P*-value.

**Supplementary Table 6 Canonical pathway enrichment in MTHFD2 network.**

<b>MTHFD2 network: Top functional canonical gene set categories</b>	<b>p-value</b>
MTOR_UP.N4.V1_UP	5.35E-13
ALK_DN.V1_UP	2.23E-11
GO_CELLULAR_AMINO_ACID_METABOLIC_PROCESS	7.32E-08
KEGG_GLYCINE_SERINE_AND_THREONINE_METABOLISM	2.53E-06
REACTOME_CYTOSOLIC_TRNA_AMINOACYLATION	2.53E-06
GO_SERINE_FAMILY_AMINO_ACID_METABOLIC_PROCESS	2.53E-06
GO_TRNA_BINDING	2.53E-06
HALLMARK_MTORC1_SIGNALING	3.91E-06
GO_INTRINSIC_APOPTOTIC_SIGNALING_PATHWAY_IN_RESPONSE_TO_ENDOPLASMIC_RETICULUM_STRESS	6.39E-06
GO_ORGANIC_ACID_METABOLIC_PROCESS	7.46E-06
KEGG_AMINOACYL_TRNA_BIOSYNTHESIS	1.08E-05
REACTOME_TRNA_AMINOACYLATION	1.08E-05

The top 12 canonical gene sets (p-value) are shown. *MTOR* = mechanistic Target of Rapamycin, *ALK* = Anaplastic Lymphoma Kinase, *MTORC1* = MTOR complex 1.



**Supplementary Table 7: Clinical and demographic data of the human atherosclerosis cohort.**

<b>Characteristics</b>	<b>Healthy</b>	<b>Patients</b>
<b>Demographic data</b>		
No	20	52
Mean age (range)	65 (50–82)	68.7 (52–80)
Male /female	10/10	32/20
Smokers	0	4
<b>Clinical data</b>		
Hypertension	0	32
Diabetes	0	0
Hyperlipidemia	0	50
Coronary disease	0	12
Myocardial Infraction	0	0
Valve insufficiency	0	0
Renal disease	0	0
Heart failure	0	0
<b>Angiographic carotid stenosis</b>		
<90%	0	52
<b>Plaque histopathology</b>		
Unstable	0	26
Stable	0	26
<b>Medication</b>		
ACE inhibitors	0	16
β-blockers	0	14

**Supplementary Table 8: Characteristics of the HDL study population.**

	Healthy (n=10)	CAD (n=10)	p-value
Number of male subjects	10	10	
Age	55 ± 10	62 ± 7	0.1384
BP systolic (mmHg)	124 ± 10	131 ± 18	0.3330
BP diastolic (mmHg)	83 ± 6	80 ± 11	0.5775
Heart rate (bpm)	57 ± 7	68 ± 15	0.0599
LVEF (%)	60 ± 5	57 ± 7	0.2785
Glucose (mmol/l)	5 ± 0.6	6.7 ± 1.5	0.0406
HbA1c (%)	5.4 ± 0.1	6.2 ± 1.1	0.0051
Total cholesterol (mmol/l)	5.2 ± 0.8	4.2 ± 1.4	0.0607
HDL cholesterol (mmol/l)	1.5 ± 0.4	1.1 ± 0.4	0.0235
LDL cholesterol (mmol/l)	3.2 ± 0.7	2.5 ± 1.1	0.0903
Triglycerides (mmol/l)	1.0 ± 0.2	1.8 ± 1.4	0.0864
Creatinine (µmol/l)	83.5 ± 12.1	82.7 ± 29.8	0.9383
NT-proBNP (ng/l)	46.8 ± 32.9	408.4 ± 524.7	0.0432
Leukocytes (10 <sup>6</sup> /microl)	5 ± 0.8	6.7 ± 1.3	0.0031
Erythrocytes (10 <sup>6</sup> /microl)	4.9 ± 0.3	4.7 ± 0.3	0.2811
Hemoglobin (g/dl)	145.2 ± 5.3	141.1 ± 10	0.2685
Thrombocytes (10 <sup>6</sup> /µl)	223.5 ± 90.4	213.9 ± 44.7	0.7668
Hypertension	0	9	
Diabetes	0	2	
Obesity	0	7	
Dyslipidemia	0	10	
MI History	1	2	

BMI = body mass index, LVEF = left ventricular ejection fraction, BP = blood pressure, NT-proBNP = N-terminal pro brain natriuretic peptide, CK = creatine kinase, MI = myocardial infarction. Data are represented as mean ± SD (Student's t-test).

## Supplementary Table 9: List of primers for RT-qPCR.

### List of Human Primers

Name	Forward Primer (5'-3')	Reverse Primer (5'-3')
$\beta$ -Actin	AAAGACCTGTACGCCAACAC	GTCATACTCCTGCTTGCTGAT
MTHFD2	GATCCTGGTTGGCGAGAATCC	TCTGGAAGAGGCAACTGAACA
SHMT2	CCCTTCTGCAACCTCACGAC	TGAGCTTATAGGGCATAGACTCG
PHGDH	CTGCGGAAAGTGCTCATCAGT	TGGCAGAGCGAACAATAAGGC
PSAT1	TGCCGCACTCAGTGTGTTAG	GCAATTCCCGCACAAAGATTCT
MTHFD1L	CTGCCTTCAAGCCGGTTCTT	TTTCCTGCATCAAGTTGTCGT
GARS	ATGGAGGTGTTAGTGGTCTGT	CTGTTCCCTCTTGATAAAGTGCT
CARS	GGTGACGTGGTATTGCTGTG	CTCTTCTCCCGATACTGCTCG
CEBPB	ACAAGCACAGCGACGAGTACAAGA	TGCTTGAACAAGTTCCGCAGGGT
SLC7A5	CCGTGAACTGCTACAGCGT	CTTCCCGATCTGGACGAAGC
SLC7A1	GTCCTGCTCAACATTGGGCA	CAGGGCCTGCATTCTCAGC
ASNS	GGAAGACAGCCCCGATTTACT	AGCACGAACTGTTGTAATGTCA
DDIT3	AGCTGGAAGCCTGGTATGAG	AGTCAGCCAAGCCAGAGAAG
ATF4	CTGCCCGTCCCAAACCTTAC	TGCTCCGCCCTCTTCTTCTG
PCK2	GCCATCATGCCGTAGCATC	AGCCTCAGTTCATCACAGAT
PFKFB3	GGGCCAAAGCTGACCAACTC	CCCTTCTTTCCGCAGGTAGC
G6PD	CGAGGCCGTCACCAAGAAC	GTAGTGGTCGATGCGGTAGA
EHHADH	AAACTCAGACCCGGTTGAAGA	TTGCAGAGTCTACGGGATTCT
CTH	GGCCTGGTGTCTGTAAATTGT	GCCATTCCGTTTTTTGAAATGCT
CBS	GGCCAAGTGTGAGTTCTTCAA	GGCTCGATAATCGTGTCCCC
F3	GGAACCCAAACCCGTCAATC	GCCAAGTACGTCTGCTTAC
KDM7A	ACCTGAATGGAGAGCGAAAG	TCATGTTCCACTCCCTCTAC
GSS	GGGAGCCTCTTGCAGGATAAA	GAATGGGGCATAGCTCACCAC
sXBP1	CCGCAGCAGGTGCAGG	GAGTCAATACCGCCAGAATCCA
GCLM	CATTACAGCCTTACTGGGAGG	ATGCAGTCAAATCTGGTGGA
18srRNA	CTTTGGTCGCTCGCTCCTC	CTGACCGGGTTGGTTTTGAT

### List of Mouse Primers

Name	Forward Primer (5'-3')	Reverse Primer (5'-3')
Mthfd2	GCCCAAATTGGTTGGAGATG	CGCTGTTTGGACTTGAACAC
Phgdh	ATGGCCTTCGCAAATCTGC	AGTTCAGCTATCAGCTCCTCC
Shmt2	TGGCAAGAGATACTACGGAGG	GCAGGTCCAACCCCATGAT
Slc3a2	TGATGAATGCACCCTTGACTTG	GCTCCCCAGTCAAAGTGGA

## List of Zebrafish Primers

<b>Name</b>	<b>Forward Primer (5'-3')</b>	<b>Reverse Primer (5'-3')</b>
elfa	CTTCTCAGGCTGACTGTGC	CCGCTAGCATTACCCTCC
mthfd2	CGGGCATTGCGGAAACTCTG	CTGGCTGGATTGTCACCTAC